An Integrated 2-D and 1-D Model of Hydrodynamic and Water Quality

Yan Wu - Hyder Consulting

Roger Falconer and Binliang Lin - School of Engineering, Cardiff University

INTRODUCTION

In modelling estuarine and riverine processes, the modelling domain often covers areas of a different physical nature, e.g. large water basins with two-dimensional flow structure and narrow meandering channels with one-dimensional flow structure. When a two-dimensional model is used for such cases the detail bathymetric features of a narrow meandering channel are lost unless a very fine grid system is used, which will increase the computing burden dramatically. Whilst if a one-dimensional model is adopted then the two-dimensional flow features in the wider part of an estuary or river are not resolved.

For many engineering problems the physical processes are involved in both estuarine and riverine waters. Therefore, a combined 2-D and 1-D model for predicting accurately water flows, physical transport processes and the chemical processes of heavy metals between their dissolved and particulate phases in the estuarine and riverine waters is in demand. The common approach is to use a 2-D and 1-D overlapping model, which explicitly exchanges the data between its 2-D and 1-D models for their boundary conditions over the overlapping zone (Lin et al, 2001). The models based on the explicit approach are generally mass non-conservative and often subject to numerical instability.

In this paper, a model dynamically integrating a two-dimensional depth-integrated model and a one-dimensional cross-sectional averaged model, is described. The present integrated model, which implicitly solves the 2-D and 1-D system as a whole, eliminates the explicit exchange of data between 2-D and 1-D models for their boundary conditions, and is fully mass conservative. The model was applied to predict flows as well as salt, cohesive sediment and heavy metal transport processes in the Mersey Estuary. A modified ULTIMATE QUICKEST scheme (Wu and Falconer, 1998) was used in the model to achieve accurate and numerical oscillation-free solutions. The model was first calibrated against six sets of data, collected during spring and neap tidal cycles, for water level, salinity and suspended sediment. The calibrated model was then used to investigate heavy metal transport processes in the estuary with the partitioning coefficient between the dissolved and absorbed particulate phases being modelled as a function of salinity. Comparisons between the model predictions and field-measured data along the estuary were also made.

MATHEMATICAL MODEL

Hydrodynamic Models

The hydrodynamic model used to predict the water elevations and velocity fields in coastal, estuarine and riverine waters initially involved the solution of the governing equations of fluid flow. The two-dimensional hydrodynamic equations are generally based on the depth-integrated 3-D Reynolds equations for incompressible and unsteady turbulent flows, with the effects of the earth's rotation, bottom friction and wind shear being included (see Falconer, 1993):-

$$\frac{\partial z}{\partial t}+\frac{\partial Q_x}{\partial x}+\frac{\partial Q_y}{\partial y}=0 \tag{1}$$

$$\frac{\partial Q_x}{\partial t}+b\frac{\partial UQ_x}{\partial x}+b\frac{\partial VQ_x}{\partial y}=fQ_y-gH\frac{\partial z}{\partial x}+\frac{t_{xw}}{r}-\frac{t_{xb}}{r}+\bar{e}H\left[\frac{\partial^2 U}{\partial x^2}+\frac{\partial^2 U}{\partial y^2}\right] \tag{2}$$

$$\frac{\partial Q_y}{\partial t}+b\frac{\partial UQ_y}{\partial x}+b\frac{\partial VQ_y}{\partial y}=-fQ_x-gH\frac{\partial z}{\partial y}+\frac{t_{yw}}{r}-\frac{t_{yb}}{r}+\bar{e}H\left[\frac{\partial^2 V}{\partial x^2}+\frac{\partial^2 V}{\partial y^2}\right] \tag{3}$$

where z = water elevation above (or below) datum; U, V = depth averaged velocity components in x, y directions; $Q_x = UH$, $Q_y + VH$ = unit width discharge components in x, y directions; $H = z + h$ =

total water depth, h = water depth below datum; b = momentum correction factor; f = Coriolis parameter; t_{xw}, t_{yw} = surface wind shear stress components in x, y directions; t_{xb}, t_{yb} = bed shear stress components in x, y directions, with Chezy value being determined by Colebrook-White equation for a given bed roughness length; and $\bar{e}$ = depth average eddy viscosity.

The one-dimensional governing hydrodynamic equations describing flows in rivers are based on the St Venant equations known as hydraulic principles in hydraulic engineering for 1-D unsteady open channel flow. Various forms of the St Venant equations were introduced in the field of unsteady open channel flow since 1950's when the electronic computer was developed. The most often used form in practice can be written as (Cunge et al, 1980):-

$$T\frac{\partial z_R}{\partial t}+\frac{\partial Q_R}{\partial x}=0 \tag{4}$$

$$\frac{\partial Q_R}{\partial t}+\frac{\partial}{\partial x}\left(b\frac{Q_R^2}{A}\right)+gA\frac{\partial z_R}{\partial x}+g\frac{Q_R|Q_R|}{C^2AR}=0 \tag{5}$$

where T = top width of the channel; z_R = water elevation above (or below) datum; Q_R = discharge; b = momentum correction factor due to the non-uniform in the cross section; g = acceleration due to gravity; A = wetted cross-sectional area; C = Chezy coefficient; $R = A/P$ = hydraulic radius, P = wetted perimeter of the cross-section.

Water Quality Models

Salt transport

Salinity, the salt content of water, is an important factor in the spatial dynamics of estuarine fisheries. It plays an important role in heavy metal partitioning between the dissolved and particulate phases and in turn influences the distribution of heavy metals in estuaries. Salinity may also affect flocculation processes of cohesive particles. As a conservative content, salinity distributions in estuaries can be modelled by the advection-diffusion equation.

2-D depth-integrated advection-diffusion equation:-

$$\frac{\P SH}{\P t}+\frac{\P SUH}{\P x}+\frac{\P SVH}{\P y}-\frac{\P}{\P x}\left[HD_x\frac{\P S}{\P x}\right]-\frac{\P}{\P y}\left[HD_y\frac{\P S}{\P y}\right]=0 \tag{6}$$

where S = depth-averaged salinity; D_x, D_y = depth-averaged dispersion coefficients in x, y directions respectively, which can be calculated as Preston (1985).

1-D cross-sectional averaged advection-diffusion equation:-

$$\frac{\P SA}{\P t}+\frac{\P SU_RA}{\P x}-\frac{\P}{\P x}\left[AK_x\frac{\P S}{\P x}\right]=0 \tag{7}$$

where S = cross-sectional averaged salinity; $U_R = Q_R/A$ = cross-sectional averaged velocity; K_x = longitudinal dispersion coefficient.

Sediment transport

The heavily contaminated sediments, resulting from industrial and municipal effluents, accidental oil spills etc, could release heavy metals, mineral oils and other toxic contaminants. This desorption of contaminants from their particulate phase can impact significantly on the ecological balance of estuarine and riverine waters. Therefore, understanding and determining sediment dynamics is of vital importance for the environmental management of estuaries and rivers.

The two-dimensional governing equation describing sediment transport processes can be written as:-

$$\frac{\P SH}{\P t}+\frac{\P SUH}{\P x}+\frac{\P SVH}{\P y}-\frac{\P}{\P x}\left[HD_x\frac{\P S}{\P x}\right]-\frac{\P}{\P y}\left[HD_y\frac{\P S}{\P y}\right]=\begin{cases}q_{ero}+q_{dep}, & cohesive\ sediment\\ w_s(S_{ae}-S), & non-cohesive\ sediment\end{cases} \tag{8}$$

where S = depth-averaged sediment concentration; q_{dep}, q_{ero} = cohesive sediment deposition and erosion rates respectively, which may be obtained using empirical expressions of Krone (1962); w_s = sediment settling velocity; S_{ae} = equilibrium reference sediment concentration, which can be calculated from the expression given by van Rijn (1984).

The one-dimensional cross-sectional averaged sediment transport equation can be written as:-

$$\frac{\partial SA}{\partial t}+\frac{\partial SU_R A}{\partial x}-\frac{\partial}{\partial x}\left[AK_x\frac{\partial S}{\partial x}\right]=\begin{cases}q_{ero}+q_{dep}, & cohesive\ sediment\\ w_s(S_{ae}-S)T, & non-cohesive\ sediment\end{cases} \quad (9)$$

where S = cross-sectional averaged sediment concentration; q_{dep}, q_{ero} = the deposition and erosion rates of unit length of the channel; T is top width of the channel.

Heavy metal transport

Heavy metals can exist in both the dissolved or absorbed particulate phases in estuaries. The distribution between these two phases can be defined as:-

$$K_D=\frac{P}{C} \quad (10)$$

where K_D = partitioning coefficient which is generally a function of salinity and pH (Turner and Millward, 1994); P = concentration of heavy metals adsorbed on suspended sediments; C = concentration of heavy metals dissolved in the water column.

Instead of solving the advection-diffusion equation for dissolved and absorbed particulate phases individually, An advection-diffusion equation for the total heavy metal was used to solve the total heavy metal fluxes first. And then the dissolved and absorbed particulate phases were calculated using the partition relationship (10). The 2-D transport equation governing the total heavy metal flux can be written as (Wu and Falconer, 2001):-

$$\frac{\partial C_T H}{\partial t}+\frac{\partial C_T UH}{\partial x}+\frac{\partial C_T VH}{\partial y}-\frac{\partial}{\partial x}\left[HD_x\frac{\partial C_T}{\partial x}\right]-\frac{\partial}{\partial y}\left[HD_y\frac{\partial C_T}{\partial y}\right]$$
$$+\frac{\partial}{\partial x}\left[HD_xS\frac{\partial P}{\partial x}\right]+\frac{\partial}{\partial y}\left[HD_yS\frac{\partial P}{\partial y}\right]=H(S_o^d+S_o^p)+S_b^p \quad (11)$$

where S = depth-averaged sediment concentration; S_o^d = source or sink of dissolved heavy metal; S_o^p = source or sink of absorbed particulate heavy metal; S_b^p = source term from or to bed with sediments by erosion and deposition; C_T = concentration of total heavy metal, i.e.:-

$$C_T=C+SP \quad (12)$$

Substituting the partitioning equation (10) into equation (12) gives:-

$$C=\frac{C_T}{1+K_DS} \quad (13)$$

The 1-D cross-sectional averaged equation describing the total heavy metal transport processes can be written as:-

$$\frac{\partial C_T A}{\partial t}+\frac{\partial C_T U_R A}{\partial x}-\frac{\partial}{\partial x}\left[AK_x\frac{\partial C_T}{\partial x}\right]+\frac{\partial}{\partial x}\left[AK_xS\frac{\partial P}{\partial x}\right]=A(S_o^d+S_o^p)+S_b^P \quad (14)$$

NUMERICAL METHODS

Hydrodynamic Models

Two-dimensional depth-averaged model

The two-dimensional depth-averaged hydrodynamic equations are discretized using an alternating direction implicit scheme based on the finite difference method. A space-staggered grid is used, with the velocities and depths being located at the centre of the sides of the grid cell and the other variables located at the centre of the grid cell. For the first half-time step the continuity equation (1) and x direction momentum equation (2) are discretized, and the following tri-diagonal equations are obtained (for details, see Falconer, 1986):-

$$a_i Q_x\Big|_{i-\frac{1}{2},\,j}^{n+\frac{1}{2}}+b_i z_{i,\,j}^{n+\frac{1}{2}}+c_i Q_x\Big|_{i+\frac{1}{2},\,j}^{n+\frac{1}{2}}=A_i \quad (15)$$

$$d_i z_{i,\,j}^{n+\frac{1}{2}}+e_i Q_x\Big|_{i+\frac{1}{2},\,j}^{n+\frac{1}{2}}+f_i z_{i+1,\,j}^{n+\frac{1}{2}}=B_i \quad (16)$$

With appropriate boundary conditions the above tri-diagonal equations can be solved using the method of Gauss elimination and back substitution (or Thomas algorithm).

Similarly, for the second half time step, the continuity equation (1) and y direction momentum equation (3) are solved.

One-dimensional cross-sectional averaged model

A space-staggered grid, with the discharges being located at the sides of the grid cell (segment) and the water elevation located at the centre of the grid cell, is used to discretized the one-dimensional cross-sectional averaged hydrodynamic equations (4) and (5). The finite volume approach is used to derive the discretized equations.

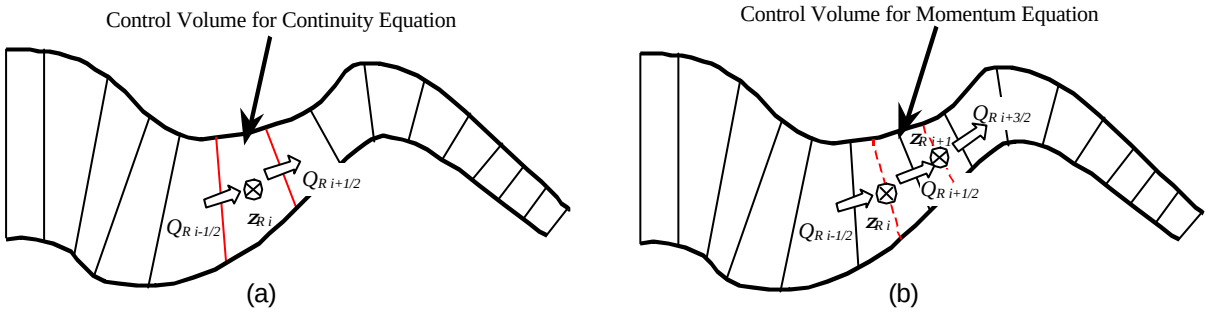

Figure 1: Staggered Grid and Control Volumes for Continuity and Momentum Equations

For the continuity equation (4) the control volume as shown in Figure 1(a) is adopted, and the following discretized continuity equation is obtained:-

$$a_i Q_R\Big|_{i-\frac{1}{2}}^{n+\frac{1}{2}} + b_i z_R\Big|_i^{n+\frac{1}{2}} + c_i Q_R\Big|_{i+\frac{1}{2}}^{n+\frac{1}{2}} = A_i \qquad (17)$$

where $a_i = -\frac{\Delta t}{2}$, $b_i = T_i^n\left(s_{i+\frac{1}{2}} - s_{i-\frac{1}{2}}\right)$, $c_i = \frac{\Delta t}{2}$, $A_i = T_i^n\left(s_{i+\frac{1}{2}} - s_{i-\frac{1}{2}}\right) z_R\Big|_i^{n-\frac{1}{2}} - \frac{\Delta t}{2}\left(Q_R\Big|_{i+\frac{1}{2}}^{n-\frac{1}{2}} - Q_R\Big|_{i-\frac{1}{2}}^{n-\frac{1}{2}}\right)$

For the momentum equation (5) the control volume as shown in Figure 1(b) is used to get the following discretized quation:-

$$d_i z_R\Big|_i^{n+\frac{1}{2}} + e_i Q_R\Big|_{i+\frac{1}{2}}^{n+\frac{1}{2}} + f_i z_R\Big|_{i+1}^{n+\frac{1}{2}} = B_i \qquad (18)$$

where $d_i = -\frac{g A_{i+\frac{1}{2}}^n \Delta t}{2(s_{i+1} - s_i)}$, $e_i = 1 + \frac{g\Delta t \left|Q_R\right|_{i+\frac{1}{2}}^{n-\frac{1}{2}}\Big|}{\left(C_{i+\frac{1}{2}}^n\right)^2 A_{i+\frac{1}{2}}^n R_{i+\frac{1}{2}}^n}$, $f_i = \frac{g A_{i+\frac{1}{2}}^n \Delta t}{2(s_{i+1} - s_i)}$

$$B_i = Q_R\Big|_{i+\frac{1}{2}}^{n-\frac{1}{2}} - \frac{b\Delta t}{s_{i+1} - s_i}\left[\frac{\left(Q_R\Big|_{i+1}^n\right)^2}{A_{i+1}^n} - \frac{\left(Q_R\Big|_i^n\right)^2}{A_i^n}\right] - \frac{g A_{i+\frac{1}{2}}^n \Delta t}{2(s_{i+1} - s_i)}\left(z_R\Big|_{i+1}^{n-\frac{1}{2}} - z_R\Big|_i^{n-\frac{1}{2}}\right)$$

Equations (17) and (18) construct a tri-diagonal equation system, and can be solved using the method of Gauss elimination and back substitution with appropriate boundary conditions.

Dynamically integrated 2-D and 1-D model

The dynamically integrated 2-D and 1-D model is constructed on a combined 2-D and 1-D grid system. The one-dimensional grid can be connected with two-dimensional grid in x direction or y direction.

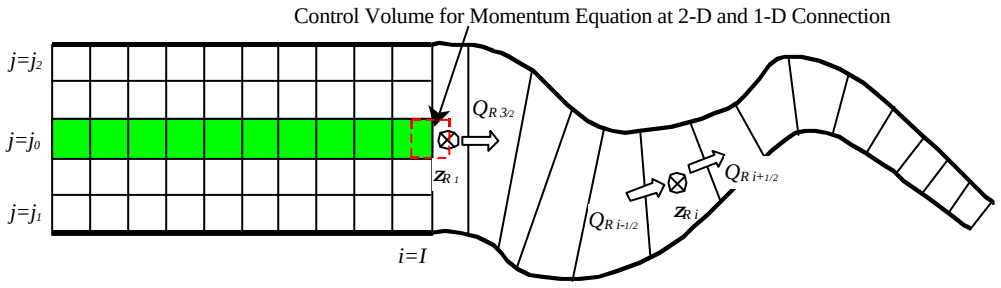

Figure 2: Combined 2-D and 1-D Grid System of Dynamically Integrated Model

To solve implicitly two-dimensional and one-dimensional systems together, one of grid rows in two-dimensional grid system has to be chosen as a principal grid row (i.e. the green grid row as shown in Figure 2), which connects with the one-dimensional grid system. During the calculation the principal rows, i.e. the rows connecting with one-dimensional grid systems, are always calculated first, and then the other rows in two-dimensional grid system are calculated. The numerical scheme is described as below.

For the cells on the principal grid row, the discretized equations have the following form:-

$$a_i Q_x\Big|_{i-\frac{1}{2},\ j_0}^{n+\frac{1}{2}} + b_i z_{i,\ j_0}^{n+\frac{1}{2}} + c_i Q_x\Big|_{i+\frac{1}{2},\ j_0}^{n+\frac{1}{2}} = A_i \qquad i = 1, 2, 3 \ldots I \tag{19}$$

$$d_i z_{i,\ j_0}^{n+\frac{1}{2}} + e_i Q_x\Big|_{i+\frac{1}{2},\ j_0}^{n+\frac{1}{2}} + f_i z_{i+1,\ j_0}^{n+\frac{1}{2}} = B_i \qquad i = 1, 2, 3 \ldots I-1 \tag{20}$$

where I is the total number of the cells on the principal grid row.

Based on the control volume shown as in Figure 2, the discretized momentum equation at the connecting point of 2-D grid $i = I + \frac{1}{2},\ j = j_0$ can be derived as:-

$$d_I z_{I,\ j_0}^{n+\frac{1}{2}} + e_I Q_x\Big|_{I+\frac{1}{2},\ j_0}^{n+\frac{1}{2}} + f_I z_R\Big|_1^{n+\frac{1}{2}} = B_I \tag{21}$$

where

$$d_I = -\frac{gH_{I+\frac{1}{2},\ j_0}^n}{\Delta x + \left(s_{3/2} - s_{1/2}\right)}, \quad e_I = \frac{1}{\Delta t} + \frac{g\left|Q_x\right|_{i+\frac{1}{2},\ j_0}^n}{2\left(H_{I+\frac{1}{2},\ j_0}^n C_{I+\frac{1}{2},\ j_0}^n\right)^2}, \quad f_I = \frac{gH_{I+\frac{1}{2},\ j_0}^n}{\Delta x + \left(s_{3/2} - s_{1/2}\right)}$$

$$B_I = \frac{Q_x\Big|_{I+\frac{1}{2},\ j_0}^{n-\frac{1}{2}}}{\Delta t} - b\left[\frac{(UQ)_{I+1,\ j_0}^n - (UQ_x)_{I,\ j_0}^n}{\Delta x + \left(s_{3/2} - s_{1/2}\right)}\right] - \frac{gH_{I+\frac{1}{2},\ j_0}^n}{\Delta x + \left(s_{3/2} - s_{1/2}\right)}\left(z_R\Big|_1^{n-\frac{1}{2}} - z_{I,\ j_0}^{n-\frac{1}{2}}\right) - \frac{gQ_x\Big|_{I+\frac{1}{2},\ j_0}^{n-\frac{1}{2}}\left|Q_x\right|_{I+\frac{1}{2},\ j_0}^{n-\frac{1}{2}}}{2\left(H_{I+\frac{1}{2},\ j_0}^n C_{I+\frac{1}{2},\ j_0}^n\right)^2}$$

The discretized continuity equation at the connecting point can be obtained using the first segment of one-dimensional system as the control volume:-

$$a_{I+1} Q_x\Big|_{I+\frac{1}{2},\ j_0}^{n+\frac{1}{2}} + b_{I+1} z_R\Big|_1^{n+\frac{1}{2}} + c_{I+1} Q_R\Big|_{3/2}^{n+\frac{1}{2}} = A_{I+1} \tag{22}$$

where

$$a_{I+1} = -\frac{\Delta x \Delta t}{2}, \quad b_{I+1} = T_1^n\left(s_{3/2} - s_{1/2}\right), \quad c_{I+1} = \frac{\Delta t}{2}$$

$$A_{I+1} = T_1^n\left(s_{3/2} - s_{1/2}\right) z_R\Big|_1^{n-\frac{1}{2}} - \frac{\Delta t}{2}\left(Q_R\Big|_{3/2}^{n-\frac{1}{2}} - \Delta x Q_x\Big|_{I+\frac{1}{2},\ j_0}^{n-\frac{1}{2}} - 2\Delta x \sum_{\substack{j=j_1 \\ j \neq j_0}}^{j=j_2} Q_x\Big|_{I+\frac{1}{2},\ j}^n\right)$$

The discretized equations for the one-diemensional grid system can be written as:-

$$d_i z_R\Big|_{i-I}^{n+\frac{1}{2}} + e_i Q_R\Big|_{i-I+\frac{1}{2}}^{n+\frac{1}{2}} + f_i z_R\Big|_{i-I+1}^{n+\frac{1}{2}} = B_i, \qquad i = I+1,\ I+2,\ ...,\ I+N_R-1 \tag{23}$$

$$a_i Q_R\Big|_{i-I-\frac{1}{2}}^{n+\frac{1}{2}} + b_i z_R\Big|_{i-I}^{n+\frac{1}{2}} + c_i Q_R\Big|_{i-I+\frac{1}{2}}^{n+\frac{1}{2}} = A_i, \qquad i = I+2,\ I+3,\ ...,\ I+N_R \tag{24}$$

where N_R is the total number of segments of the 1-D grid.

Equations (19)-(24) construct a tri-diagonal sysytem of 2-D and 1-D model which can be solved efficiently using the method of Gauss elimination and back substitution.

For the one-dimensional grid system connecting with a two-dimensional grid system in y direction, the same scheme can be used with a principal grid row along y direction being chosen to connect with the one-dimensional grid system.

Water Quality Models

The QUICKEST scheme originally developed by Leonard (1979) was used in the present model. Even though the third-order QUICKEST scheme greatly reduces the non-physical oscillations caused by numerical dispersion, this scheme still suffers from numerical oscillations near discontinuities.

Thus, the universal limiter designed for one-dimensional problems by Leonard (1991) has been used to depress the non-physical numerical oscillations. However it was found that local discontinuities were distorted when the one-dimensional universal limiter was directly used at each control volume face for the two-dimensional problem. A modified one-dimensional ULTIMATE algorithm for the two-dimensional problem has been constructed to avoid the variation of local discontinuities (Wu and Falconer, 1998).

In applying the universal limiter a criteria was used to check that the solute concentration maintained monotonicity. In estuarine and riverine flows the water depth or cross-section area may vary rapidly, thus the monotonicity of the depth integrated concentration or cross-section integrated concentration may be different from the monotonicity of the solute concentration. Therefore, when applying the modified ULTIMATE QUICKEST scheme a conservative form advection-diffusion equation of the depth-average concentration should be used. For the detail of numerical method, see Wu and Falconer (2000).

MODEL APPLICATIONS TO THE MERSEY ESTUARY

Model Set Up

The present integrated 2-D and 1-D model was set up and applied to simulate the tidal flow, salt, sediment and heavy metal distribution in the Mersey Estuary from New Brighton (seaward) to Howley Weir (landward). The model domain was represented horizontally in two grid systems, i.e. 2-D grid and 1-D grid. The 2-D grid, covering the region from New Brighton to Hale, was represented horizontally using a mesh of 216×116 uniform grid squares, each with a length of 100m. The 1-D grid covering the region from Hale to Howley Weir was represented using 80 segments, with extensive bathymetric data at each cross-section being collected during the most recent bathymetric survey conducted by HR Wallingford Ltd and APB in 1997. The reason of ending the 2-D grid at Hale is that there is a low water channel upstream of Hale, which can not be resolved by the 2-D grid. Figure 3 shows the combined 2-D and 1-D computational grid of the Mersey Estuary as used in this study.

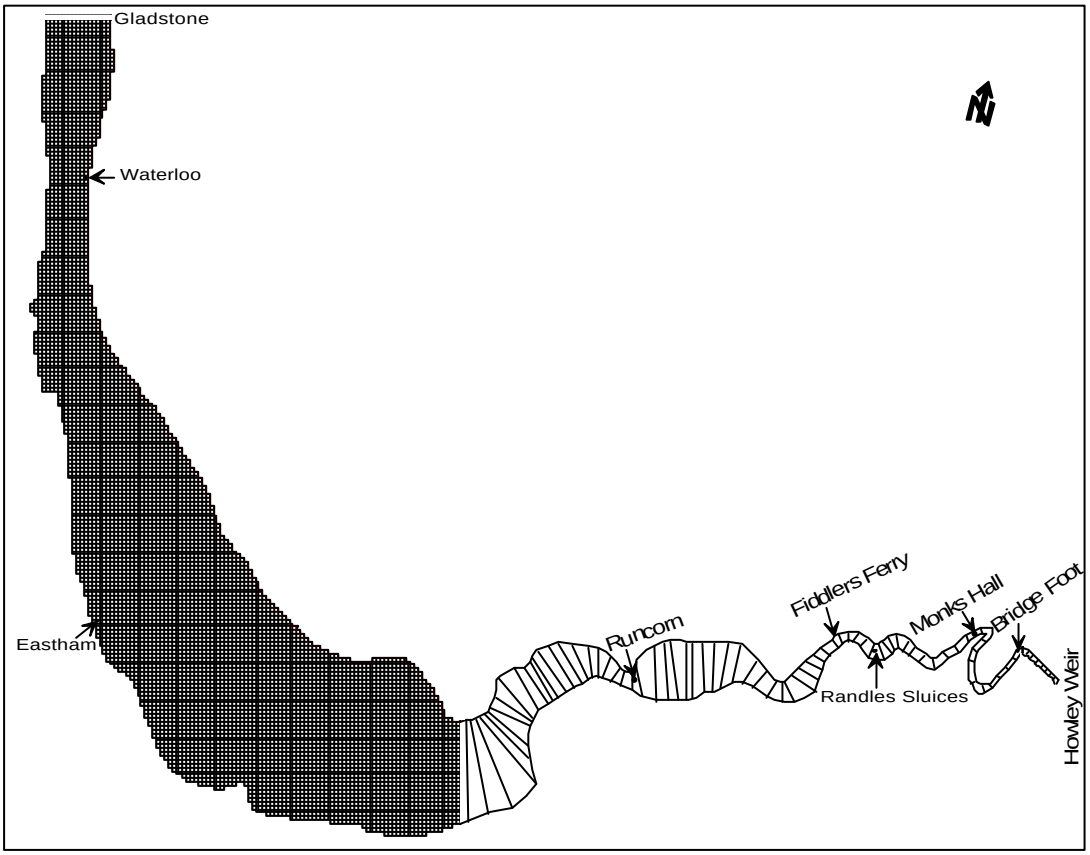

Figure 3: Combined 2-D and 1-D Grid of the Mersey Estuary and Sampling Stations

Model Calibration

The integrated model was calibrated on six sets of data provided by the Environmental Agency. Four of these data sets were collected during spring tides and two were collected during neap tides. The freshwater input from the River Mersey for these sets of data covered both wet and dry season conditions. The sampling stations are shown in Figure 3. The water elevation recorded at the Gladstone tide gauge was chosen as the seaward boundary condition to drive the tidal currents and the daily flow rate recorded at Westy was used for the upstream flow boundary condition. The bed roughness, longitudinal dispersion coefficients, critical shear stresses for sediment deposition and erosion were calibrated by trial and error. The calibrated roughness lengths were 50mm and 20mm for two regions in the two-dimensional part of the estuary. For the one-dimensional part of the estuary, the calibrated Manning coefficient was 0.02. The calibrated longitudinal dispersion and lateral diffusion constants were 800 and 1.2 respectively. Based on the data provided by the Environmental Agency the sediment grain sizes of D_{16}=12µm, D_{50}=75µm, D_{84}=195µm and D_{90}=225µm were used in the model for non-cohesive sediment. For cohesive sediment a floc size of 20µm was assumed. The calibrated critical shear stress for erosion, critical shear stress for deposition and the erosion constant were 1.0N/m^2, 0.25N/m^2 and 0.00004kg/m^{2}s respectively.

Due to the limitation of space only some calibrated results are given in this paper. Figure 4 shows the comparisons of water elevation at Waterloo, Eastham, Runcorn and Fiddlers Ferry. Figure 5 shows the comparison of the model predicted and field measured salinity over one tidal cycle at Runcorn, and Figure 6 presents the predicted and measured tidal averaged salinity along the estuary. The comparisons of model predicted suspended sediment concentrations and field data are presented in Figure 7.

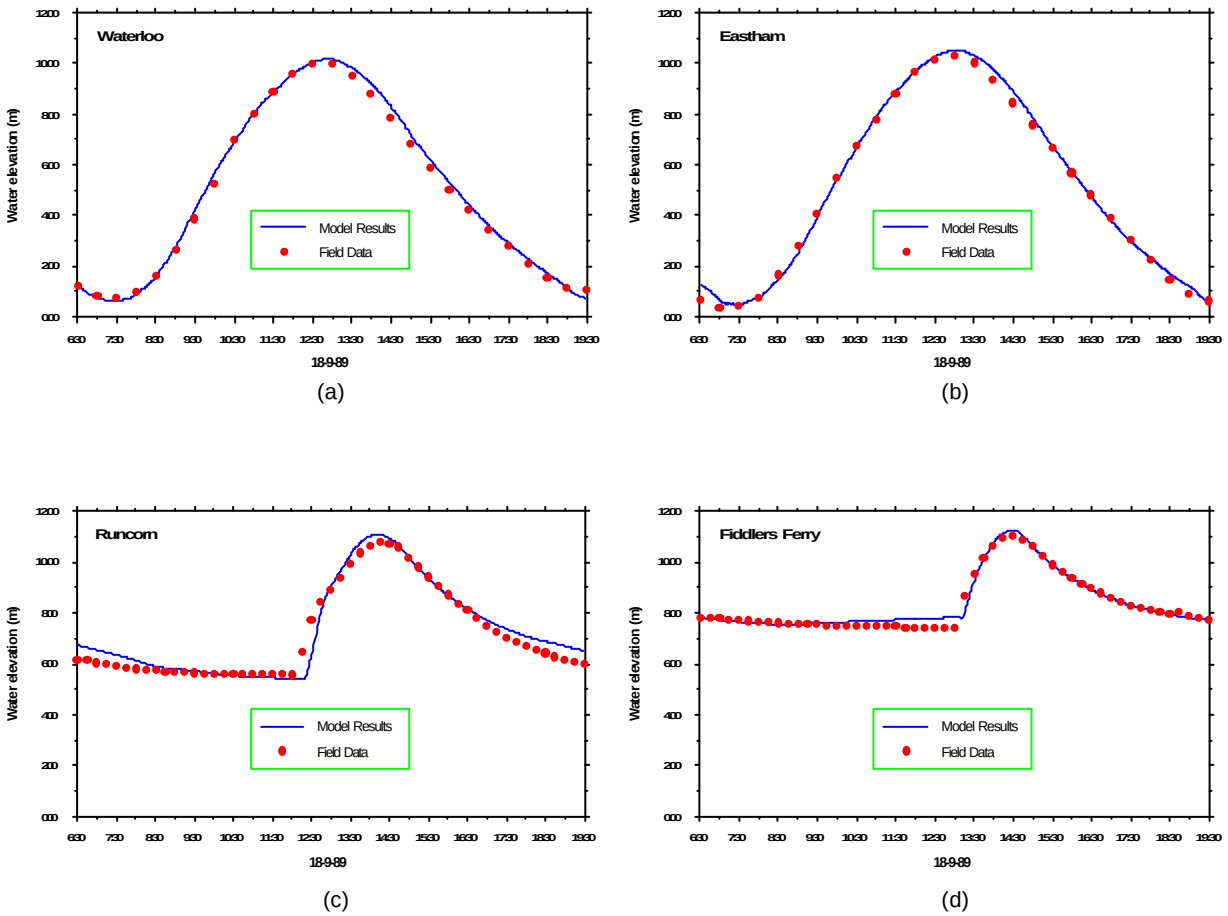

Figure 4: Comparisons of Model Predicted Water Levels with Filed Data

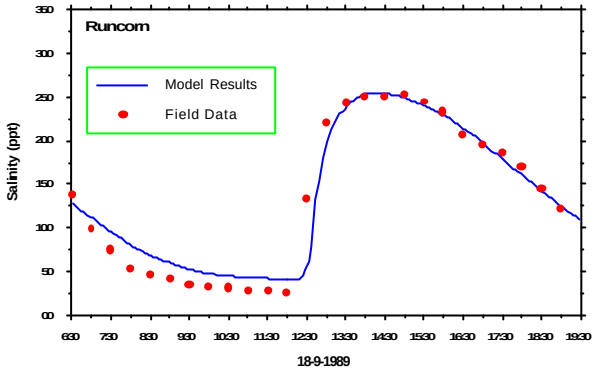

Figure 5: Salinity Time Series at Runcorn

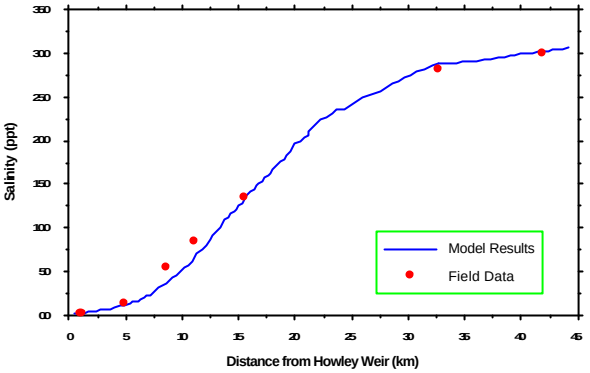

Figure 6: Salinity along the Estuary

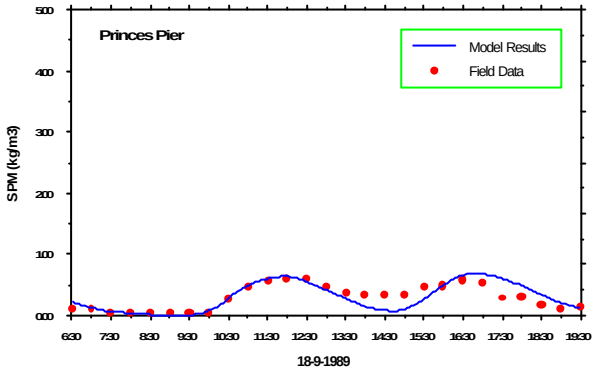

(a)

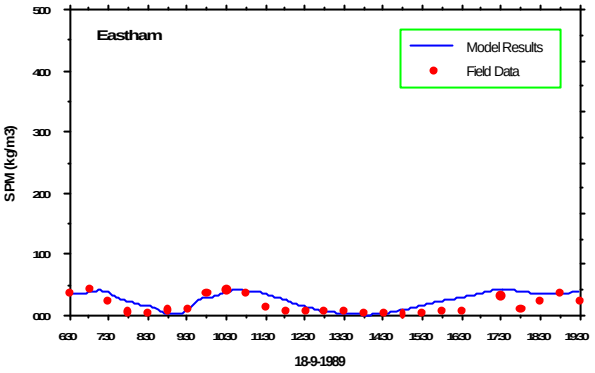

(b)

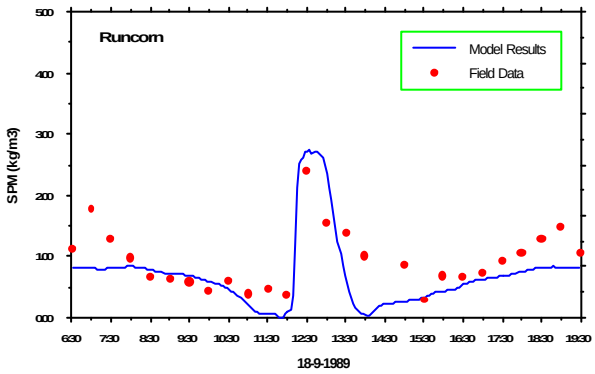

(c)

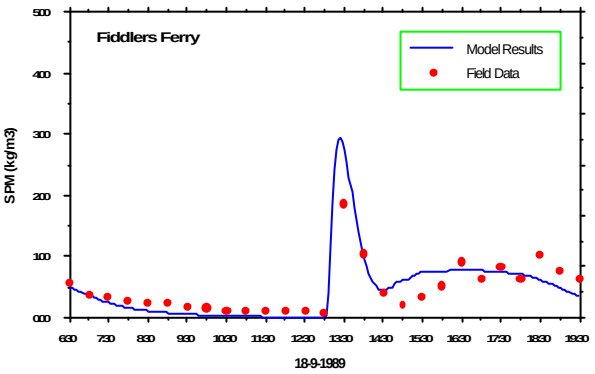

(d)

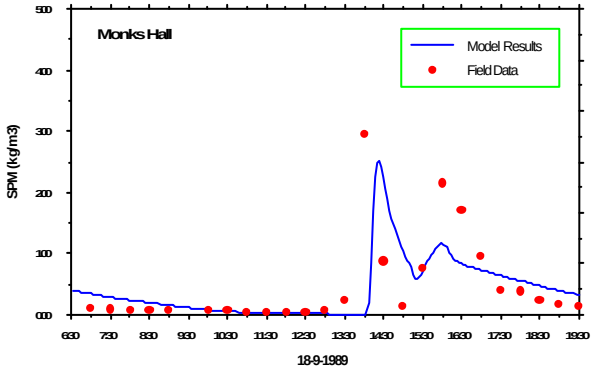

(e)

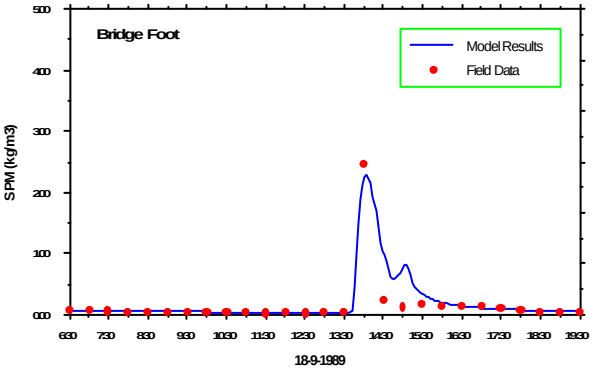

(f)

Figure 7: Comparisons of Model Predicted Suspended Sediment with Filed Data

Model Applications

The calibrated model was applied to simulate salt, cohesive sediment and cadmium transport processes in the Mersey Estuary. The partition coefficient between the dissolved and absorbed particulate phases was defined as a function of salinity. An exponential relationship between the partition coefficient and salinity (Turner and Millward, 1994) was used, with the constants in the formula being determined experimentally by the University of Plymouth.

Comparisons of the suspended sediment concentrations between the model predictions and field-measured data along the estuary are given in Figure 8. As can be seen from the results, the model predicted suspended sediment concentrations are in good agreement with the field data, except that the model under-estimated the peak for the case on 25 June. The model predicted and field-measured dissolved cadmium distributions along the estuary are shown in Figure 9. The model predicted dissolved cadmium distributions agreed well with the field data, with the absorption processes reproduced in the model predictions.

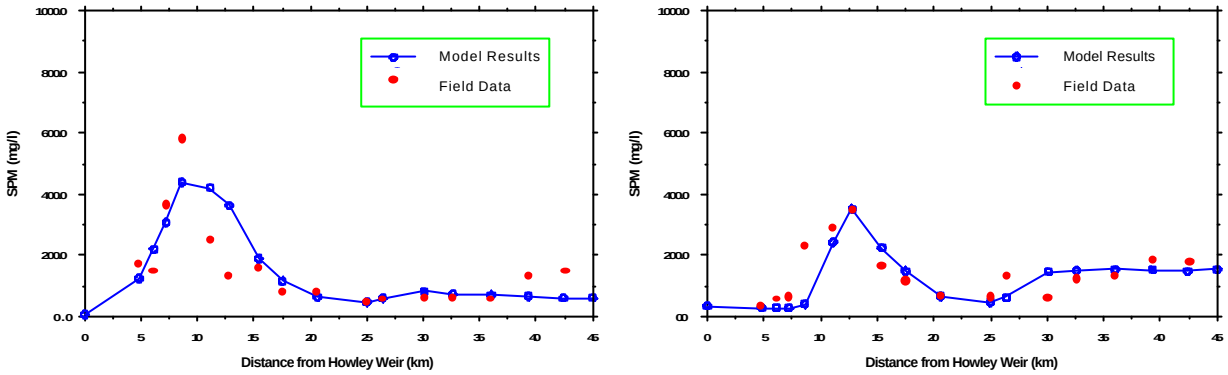

Figure 8: Comparison of Suspended Sediment Concentrations along the Estuary

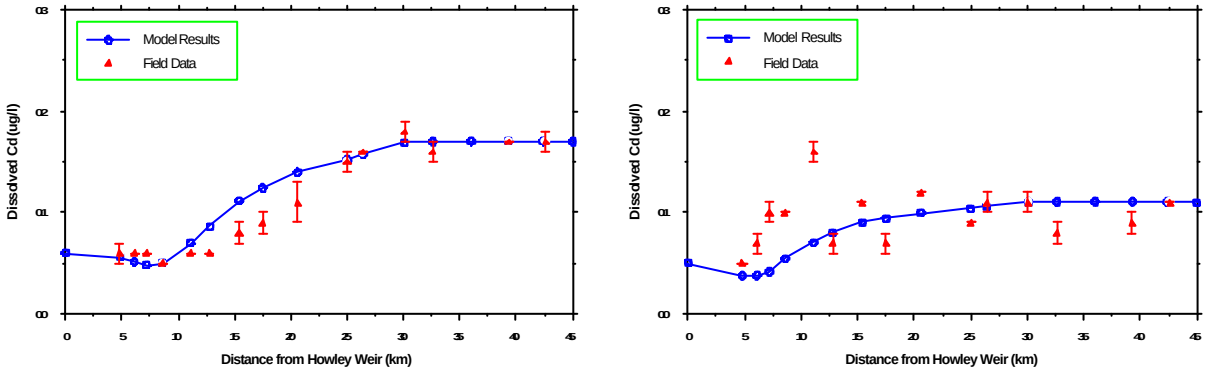

Figure 9: Comparison of Dissolved Cadmium Distributions along the Estuary

CONCLUSIONS

A dynamically integrated 2-D and 1-D model has been developed for flow and water quality modelling, with a fully mass conservative heavy metal transport module included. The present model has been calibrated and applied to study heavy metal transport processes in the Mersey Estuary. Good agreement has been obtained with the field-measured data.

ACKNOWLEDGEMENTS

The authors are grateful to the National Environment Research Council for supporting this study and to Dr. Peter Jones of Environment Agency for the provision of data. The authors are also grateful to Professor Geoff Millward of University of Plymouth for his collaboration on this project.

REFERENCES

Cunge, J.A., Holly Jr, F.M. and Verwey, A. Practical aspects of computational river hydraulics, Pitman Publishing Limited, 1980.

Falconer, R.A. A two-dimensional mathematical model study of the nitrate levels in an inland natural basin, Proceedings of the International Conference on Water Quality Modeling in the Inland Natural Environment, BHRA Fluid Engineering, Bournemouth, England, Paper J1, 325-344, 1986.

Falconer, R.A. An introduction to nearly horizontal flows, In Coastal, Estuarial and Harbor Engineers' Reference Book, Ed., M. B. Abbott & W. A. Price, pp. 27-36. E & FN Spon Ltd., London, 1993.

Leonard, B.P. A stable and accurate convective modeling procedure based on quadratic upstream interpolation. Comput. Methods Appl. Mech. Eng., **19**, 59-98, 1979.

Leonard, B.P. The ULTIMATE conservative difference scheme applied to unsteady one-dimensional advection. Comp. Methods Appl. Mech. Eng., **88**, 17-74, 1991.

Lin, B., Kashefipour, S.M., Harris E. and Falconer, R.A. Modelling flow and water quality in estuarine and riverine waters: A dynamically linked 1-D and 2-D models approach. Proceedings of XXIX IAHR Congress, Theme B: Environmental Hydraulics, 469-475, 2001.

Krone, R.B. Flume studies of the transport of sediment in estuarial processes, Final Report, Hydraulic Engineering Laboratory and Sanitary Engineering Research Laboratory, University of California, Berkeley, 1962.

Turner, A. and Millward, G.E. The partitioning of trace metals in a macrotidal eatuary: Implications for contaminant transport models. Estuarine, Coast. Shelf Sci. **39**, 45-58, 1994.

Van Rijn, L.C. Sediment transport Part 2: Suspended load transport, Journal of Hydraulic Engineering, ASCE, **110**, No. 11, 1613-1641, 1984.

Wu, Y. and Falconer, R.A. Two-dimensional ULTIMATE QUICKEST scheme for pollutant transport in free-surface flows, Third International Conference on Hydroscience and Engineering, Cottbus/Berlin, Germany, 1998.

Wu, Y. and Falconer, R.A. A mass conservative 3-D numerical model for predicting solute fluxes in estuarine waters. Advances in Water Resources, **23**, 531-543, 2000.

Wu, Y., Falconer, R. A. and Lin, B. Hydro-environmental modelling of heavy metal fluxes in an estuary. Proceedings of XXIX IAHR Congress, Theme B: Environmental Hydraulics, 732-739, 2001.